2014 IEEE International Conference on Robotics & Automation (ICRA)
Hong Kong Convention and Exhibition Center
May 31 - June 7, 2014. Hong Kong, China

Design and Control of a Low Cost 6 DOF Master Controller

Tian Qiu *Student Member IEEE,* William R. Hamel *Fellow IEEE,* Dongjun Lee *Member IEEE*

***Abstract*— This paper provides the design of a low cost master controller for teleoperation systems. The system consists of a center handle and four off the shelf haptic devices. The control law of the four devices coordinates them to provide six degree-of-freedom(DOF) force feedback. The relative position and the dimension of the handle are designed to maximize the range of motion. The system actuation redundancy problem is formulated into a standard convex optimization problem and resolved. The squared sum of the force provided by all the haptic devices are defined as the optimization function and the desired force and torque feedback is used as the linear constraints. Experiments in teleoperation and haptics projects were carried out to verify the theoretical results about system.**

I. INTRODUCTION

A haptic device with 6 DOF force feedback is essential in providing exact and complete kinesthetic feedback. There are several off-the-shelf haptics device with 6 DOF of force feedback [1], [2], [3]. Force Dimension offers several haptic devices with 6 active joints, A product called "sigma. 7" even has a seventh active grasping joint to mimic the motion of a pair of scissors[1]. Geomagic provides a haptic device called "Phantom Premium" which can provide a fairly large workspace and force capacity [3]. Another notable product called "Haptic Wand" is also available from Quanser, a research equipment company [2]. It offers five active degree of freedom with a sixth passive joint. Typically, these expensive systems that many researchers cannot afford.

There are two ways of building a 6 DOF haptic device: 1) designing and building the whole system from scratch [4], [5], [6], [7]; 2) integrating existing off-the-shelf haptics products with less degrees of freedom, and combining them to provide a higher degrees of freedom force feedback.

Building an advanced haptic device based on the off-the-shelf haptic devices can be very cost effective. The Novint Falcon is developed as a haptics research device and widely used as a computer gaming input. Many researchers have integrated multiple Falcons together to develope new haptic devices with higher degrees of freedom. Instructions about how to build it is provided in [8]. A device similar to it has seen application in device calibration for fingernail imaging [9].

*This work was supported by national science foundation

Tian Qiu is with the Mechanical, Aerospace and Biomedical Engineering Department, University of Tennessee, Knoxville, TN, 37996 USA e-mail: tqiu@utk.edu.

William Hamel. Ph. D., is Professor of Mechanical, Aerospace and Biomedical Engineering Department, University of Tennessee, Knoxville, TN, 37996 USA e-mail: whamel@utk.edu.

D. J. Lee is with the School of Mechanical & Aerospace Engineering, Seoul National University, 301 Engineering Bldg., Room # 1517. Gwanak-ro 599, Gwanak-gu, Seoul, Republic of Korea, 151-744. email: djlee@snu.ac.kr

The Phantom omni, another type of widely used haptic device, can also be integrated to provide advantages in force/torque feedback for various research. In [10], a simulation platform for Da Vinci remote surgery system is developed. Two Omnis equiped with hand grippers are used as master devices for the Da Vinci system, each of them controls one slave robot individually, so no kinematic coupling or force control collaboration is considered. The Omni and the Falcon have also been used in collaborative haptic tasks in [11]. The kinematics and dynamics have been studied in [12], [13].

The challenge of our work is that the system we build has actuation and kinematic redundancy. All Phantom Omni devices return is end-effector position information. The system needs to compute the handles' position and orientation based on this information. The computation includes coordinate transformation and vector computation. The force feedback from the devices also needs to be coordinated to ensure precision while minimizing the total load of the system.

The advantages of our system includes: low cost, effective force/torque feedback, more degrees of freedom in feedback and better position resolution. One Phantom Omni costs \$1500. So the total cost of our system is approximately \$1500×4=\$6000. The force feedback provided by the new system is the summation of four individual Omnis, so the maximum force feedback is four times the original device's. Also, the devices are configured in such a way that torque feedback can be provided to the operator, which is critical in many applications. For example, in the case where an operator is teleoperating a robot with an impact wrench as its end-effector, the resistive torque provided to the operator can provide them with ample information.

II. SYSTEM DESIGN AND KINEMATICS

In this section, the general design of the proposed controller is presented. Its mechanism and capacity are discussed.

A. Mechanism

Four Phantom Omni devices were used in our system as shown in Fig. 1. All of them were fixed onto the 80/20 aluminium frame with rods that are not shown in the figure. The rods were threaded and screwed onto the bottom frame. The original handles on the Omnis were removed. The handle we built was attached to the end links. The Omnis are electronically connected in cascade style using Firewire. Two Omnis are used in each cascade, so there are two cascades in total. According to the manual, each cascade can have a maximum of 20 haptic devices, so the amount of devices we

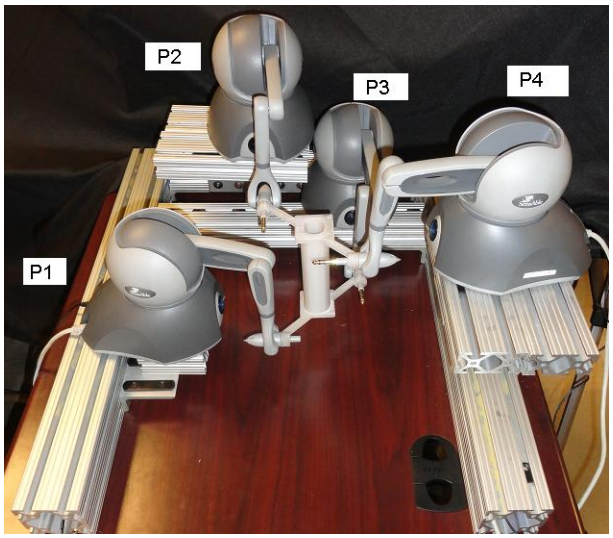

Fig. 1: 6 DOF Haptic Device

used was far below the capacity and therefore update rate would not be affected.

B. Range of Motion and Force Capacity

The haptic devices are placed to maximize the range of motion of the new master controller. The range of motion of the Phantom Omni is 6.4"× 4.8" × 2.8" (160 × 120 × 70mm) [14]. The definition of the coordinate system for a Omni is shown in Fig. 3. If the new device travels along the vertical axis, all the Omnis reach their maximum and minimum Y-axis value simultaneously, so the range of motion in Y-axis is them same as on the original Omni specifications. Comprised where there were two Omni devices, P1 and P4, were placed side ways to the other two. The range of motion on the horizontal plane is limited by the Z-axis motion of P1 and P4. Therefore, the range of motion of the new system is smaller than the Phantom Omni: 2.8'× 4.8' × 2.8' (70 × 120 × 70mm). When in the center of the workspace, the rotational range of motion of the new system is the same as the original Phantom Omni. However, it is noted that when close to the boundary of the workspace, significant rotational range of motion was lost.

The maximum exertable force of a Phantom Omni is 0.75 lbf (3.3 N)[14]. The maximum force feedback that can be offered by the proposed system is the sum of the force feedback from the four Omnis, and therefore, 3 lbf (13.2 N).

C. Handle

The handle of the new system was designed to connect the four Omnis together. It has four holes which fit tightly with each haptic device. In order to reduce its weight, the handle is hollow. The light weight is essential to because the gravity of haptic devices is added on top of the force feedback provided by the active joints. Any extra weight hampers the kinesthetic perception. 3-D printing has shown great potential in new equipment prototyping. It brings great ease to the engineers

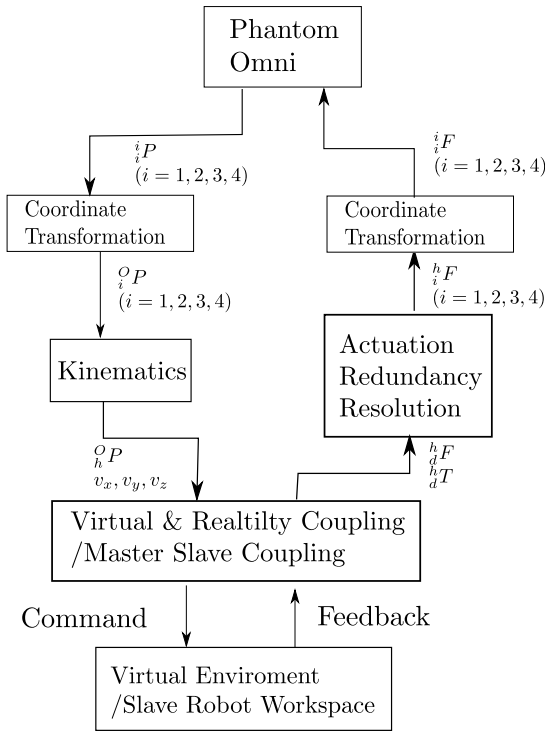

Fig. 2: Control System of the novel 6 DOF haptic device

because of the flexibility of 3-D printing. Parts coming from 3-D print are light weight and comparatively sturdy. The handle was printed using a Stratsys Fortus 250mc 3D printer.

III. Kinematics

The general control architecture of the proposed device is shown in Fig. 2. The purpose of this section is to present the solution for the "Kinematic coordinate transformation" and "Kinematic" block of that figure.

A. Kinematics of Phantom Omni

A Phantom Omni haptic device has six joints in all: three actuated and three passive. The device measures the rotation angle of each joint and computes the position of the end link. The origin of the coordinate that is attached to the end link is where the last and the second-to-last intersects. The rotational axis of the fourth link also passes through this point. The joint angles of last three passive joints effect the end effector orientation but not the position. The position and configuration data acquired from the Omnis are all with respect to its own world frame.

B. Modelling and Coordinate Transformation

Each Omni can measure the position of its end link with respect to its own world frame. We use that as the position of the corner of the handle, O_1, O_2, O_3 and O_4. Each of the coordinates corresponds to one Omni in Fig. 1. They needed to be transformed into the common world frame first.

$$ {}^{O}_{1}P = {}^{o}_{1}R^{1}_{1}P \qquad {}^{O}_{2}P = {}^{o}_{2}R^{2}_{2}P \tag{1} $$

$$ {}^{O}_{3}P = {}^{o}_{3}R^{3}_{3}P \qquad {}^{O}_{4}P = {}^{o}_{4}R^{4}_{4}P \tag{2} $$

Fig. 3: World coordinate of a Phantom Omni

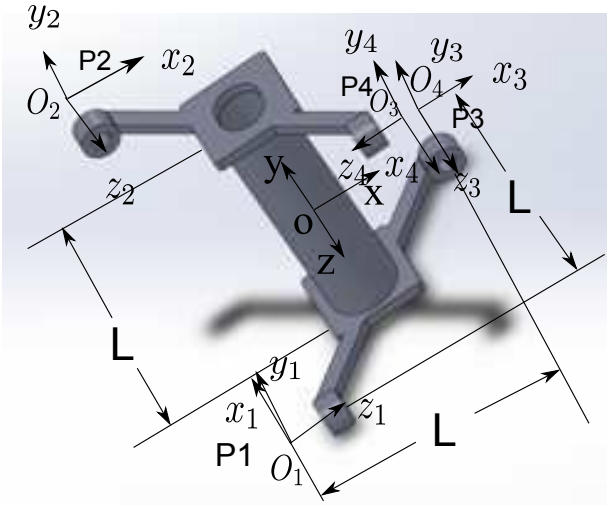

Fig. 4: Coordinate of the Handle, all of them are fixed with the handle

Since the Omni's are rigidly attached to the aluminium frame, all the coordinate transformation terms in 5 are constant homogeneous transformations. The origin of the common frame is chosen to be the world frame of Omni No. 2.

$$ {}^{o}_{1}R = \begin{bmatrix} 0 & 0 & 1 & -\frac{L}{2} \\ 0 & 1 & 0 & -\frac{L}{2} \\ -1 & 0 & 0 & \frac{L}{2} \\ 0 & 0 & 0 & 1 \end{bmatrix} \quad {}^{o}_{2}R = \begin{bmatrix} 1 & 0 & 0 & -\frac{L}{2} \\ 0 & 1 & 0 & \frac{L}{2} \\ 0 & 0 & 1 & -\frac{L}{2} \\ 0 & 0 & 0 & 1 \end{bmatrix} \tag{3} $$

$$ {}^{o}_{3}R = \begin{bmatrix} 1 & 0 & 0 & \frac{L}{2} \\ 0 & 1 & 0 & -\frac{L}{2} \\ 0 & 0 & 1 & -\frac{L}{2} \\ 0 & 0 & 0 & 1 \end{bmatrix} \quad {}^{o}_{4}R = \begin{bmatrix} 0 & 0 & -1 & \frac{L}{2} \\ 0 & 1 & 0 & \frac{L}{2} \\ 1 & 0 & 0 & \frac{L}{2} \\ 0 & 0 & 0 & 1 \end{bmatrix} \tag{4} $$

The position and orientation of the handle with respect to the center of the home position can be determined using Eq. 5. This summation and average process also reduces the position error [15].

$$ {}^{o}_{h}P = \frac{1}{4}({}^{1}_{1}P + {}^{2}_{2}P + {}^{3}_{3}P + {}^{4}_{4}P) \tag{5} $$

Where ${}^{i}_{i}P$'s are the positions of each Omni given in their own frame, and ${}^{o}_{i}R$'s are the coordinate transformation between their world frames and the common world frame. Their values are shown in Eqs. 3 and 4.

C. Kinematics

The orientation of the controller is derived using Eqs. 7, 8 and 9. All the position data (p_{1-4}) are in the common world coordinate. Therefore, only the position data from each Omni is used to derive the orientation of the handle.Thus the singularity problem that usually happens at the last three passive joints is avoided. Denote:

$$ v = [v_x, v_y, v_z] \tag{6} $$

Then,

$$ v_x = y \times z \tag{7} $$

$$ v_y = \frac{({}^{O}_{4}P - {}^{O}_{2}P) \times ({}^{O}_{3}P - {}^{O}_{1}P)}{||({}^{O}_{4}P - {}^{O}_{2}P) \times ({}^{O}_{3}P - {}^{O}_{1}P)||_2} \tag{8} $$

$$ v_z = \frac{({}^{O}_{3}P - {}^{O}_{2}P) \times ({}^{O}_{4}P - {}^{O}_{1}P)}{||({}^{O}_{3}P - {}^{O}_{2}P) \times ({}^{O}_{4}P - {}^{O}_{1}P)||_2} \tag{9} $$

The results of Eq. 7, 8 and 9 are the three unit vectors along the handle coordinate system with respect to the common world frame. When used as the column vectors, they form the orientation transformation matrix ${}^{h}_{o}R$.

IV. Force Feedback

This section addresses the "Actuation Redundancy Resolution" in Fig. 2. The actuation redundancy issue is formulated into a convex optimization problem and a solution is provided.

A. Force Coordinate Transformation

When computing the command force for each device, the desired force and torque is first represented in the frame located at the center of the handle, as shown in Fig. 4; the rest of the coordinates represented the force each Omni exerted on the handle. The reason why we pick this coordinate frame is that the leverage for each force exerted on the handle would be constant based on the chosen coordinate frame. After the optimization process, the computed force vector will be transformed into world frames of each haptic device, respectively.

B. Actuation Redundancy

The four haptic devices have three actuated joints each. Therefore, there are twelve DOF actuation in the system, but the force/torque feedback has only 6 degrees of freedom.

This actuation redundancy is formulated as an optimization problem. The objective function is the squared sum of the torque applied on each joint. The justification of this is that the torques are proportional to the current for each motor, and therefore to the power consumption of the haptic device. Minimizing the sum of the torques is the same as minimizing the effort of the whole control system and maximizing the life of the system. The constraint for this optimization problem is the desired torque and force feedback to the operator.

C. Desired Force Feedback

The desired force and torque at the new handle are given by the following equations. The subscripts stand for the index of haptic devices, the superscripts stand for the axis of the corresponding device.

$$ {}^h_dF^x = {}^h_1F^z + {}^h_2F^x + {}^h_3F^x - {}^h_4F^z; \tag{10} $$

$$ {}^h_dF^y = {}^h_1F^y + {}^h_2F^y + {}^h_3F^y + {}^h_4F^y; \tag{11} $$

$$ {}^h_dF^z = -{}^h_1F^x + {}^h_2F^z + {}^h_3F^z + {}^h_4F^x; \tag{12} $$

$$ {}^h_dT^x = (l+d)({}^h_2F^y + {}^h_3F^y) + l(-{}^h_1F^y - {}^h_4F^y) + \frac{h}{2}(-{}^h_1F^x - {}^h_2F^z + {}^h_3F^z - {}^h_4F^x) \tag{13} $$

$$ {}^h_dT^y = (l+d)(-{}^h_1F^x - {}^h_2F^x - {}^h_3F^x - {}^h_4F^x) + l({}^h_1F^z + {}^h_2F^z - {}^h_3F^z - {}^h_4F^z) \tag{14} $$

$$ {}^h_dT^z = \frac{h}{2}({}^h_2F^x - {}^h_3F^x) + l(-{}^h_1F^y + {}^h_4F^y) + l(-{}^h_2F^y + {}^h_3F^y) + \frac{h}{2}(-{}^h_1F^z - {}^h_4F^z) \tag{15} $$

Each of the four Phantoms provides 3 DOF force feedback, so the number of unknowns here is twelve. There are a total of six constraints on them, from Eq. 10 to Eq. 15. We propose an optimization function to control this redundant system. Motors in the haptic devices provide the force feedback, and forces are proportional to the currents passing through the motor. In order to minimize the load of the system, we proposed the following objective function:

$$ \min\Sigma_{i=1}^{4}(({}^h_iF^x)^2 + ({}^h_iF^y)^2 + ({}^h_iF^z)^2) = \frac{1}{2}F^TPF \tag{16} $$

where

$$ F = [{}^h_1F^x, {}^h_1F^y, {}^h_1F^z, {}^h_2F^x, {}^h_2F^y, {}^h_2F^z, {}^h_3F^x, {}^h_3F^y, {}^h_3F^z, {}^h_4F^x, {}^h_4F^y, {}^h_4F^z]^T \tag{17} $$

This function is the sum of the norm of the force feedback vectors provided by the four Omnis.

$$ P = \begin{bmatrix} 2 & 0 & 0 & 0 & 0 & 0 \\ 0 & 2 & 0 & 0 & 0 & 0 \\ 0 & 0 & 2 & 0 & 0 & 0 \\ 0 & 0 & 0 & 2 & 0 & 0 \\ 0 & 0 & 0 & 0 & 2 & 0 \\ 0 & 0 & 0 & 0 & 0 & 2 \end{bmatrix} $$

Putting Eq. 10 through Eq. 15 into matrix form and denote:

$$ b = [{}^h_dF^x, {}^h_dF^y, {}^h_dF^z, {}^h_dT^x, {}^h_dT^y, {}^h_dT^z]^T \tag{18} $$

we can get Eq. 19, where J is shown in Eq. 20. This matrix is the Jacobian matrix of the system. Since the output of the Omnis is force and the output of our new system is force and torque, the first three lines of the matrix have no dimension, and the remaining three lines have the dimension of length.

$$ JF = b \tag{19} $$

After deriving F, all the force components have to be transformed into the form with respect to the ground frame of the Omnis.

$$ {}^i_iF = {}^i_hR^h_iF \quad i = 1,2,3,4 \tag{21} $$

where ${}^i_hR$ represent the transform matrix between the handle frame and the ground frames.

D. Convex Optimization Methods

Given the objective function in Eq. 16, and linear equality constraints in Eq. 19, then apply the "Karush-Kuhn-Tucker"(KKT) condition [16], we have Eq. 22.

$$ \begin{bmatrix} P & J^T \\ J & 0 \end{bmatrix} \begin{bmatrix} F^* \\ v^* \end{bmatrix} = \begin{bmatrix} -q \\ b \end{bmatrix} \tag{22} $$

The matrix on the left side of Eq. 22 is invertible by inspection, so the optimal value can be found by directly taking the matrix inverse. Since this is a constant matrix, matrix inversion doesn't have to be processed every iteration. It can be computed offline and stored in the computer memory.

$$ v^* = -2(JJ^T)^{-1}b \tag{23} $$

$$ F^* = J^T(JJ^T)^{-1}b \tag{24} $$

Where F^* is the optimal solution for the haptic devices desired force defined in Eq. 17 and v^* is the optimal value of the dual problem [16].

V. Experiments

A. Teleoperation Experiment

In this experiment, the system we developed is used as the master robot in a teleoperation system. A Whole Arm Manipulator (WAM) robot was used as the slave robot as shown in Fig. 5. Two computers are used as the master and slave controllers. The master controller is connected to the master robot through firewire cable, and the slave controller is connected to the slave robot through Control Area Network (CAN) bus. The position, orientation and force information is transmitted between the computers through the Ethernet. 2-Channel controllers are used to enforce position and force tracking. Result of the position and orientation of the master controller is given in Fig. 6. The workspace we proposed is demonstrated. [17], [18], [19].

B. Haptics Experiment

In this experiment, the system interacts with a unilateral deformable virtual wall in virtual environment(VE). The virtual wall passes the origin and is perpendicular to the z axis. Its force and torque feedback functions are defined in Eqs. 25 and 26. The desired joint position is computed using the kinematics of the new system, the figure shows that the singularity problem is avoided because of the method we used. The force collaboration between the Omnis is shown in Fig. 7. All of them are shown in the end-effector frame of the Omnis.

$$ F = \begin{cases} k_p({}^O_hP - P_o) & z > 0 \\ 0 & z < 0 \end{cases} \tag{25} $$

$$ \tau = \begin{cases} k_t({}^O_h\theta - \theta_o) & z > 0 \\ 0 & z < 0 \end{cases} \tag{26} $$

$$J = \begin{bmatrix} 0 & 0 & 1 & 1 & 0 & 0 & 1 & 0 & 0 & 0 & 0 & -1 \\ 0 & 1 & 0 & 0 & 1 & 0 & 0 & 1 & 0 & 0 & 1 & 0 \\ -1 & 0 & 0 & 0 & 0 & 1 & 0 & 0 & 1 & 1 & 0 & 0 \\ -\frac{L}{2} & -\frac{L}{2} & 0 & 0 & \frac{L}{2} & -\frac{L}{2} & 0 & \frac{L}{2} & -\frac{L}{2} & \frac{L}{2} & -\frac{L}{2} & 0 \\ -\frac{L}{2} & 0 & \frac{L}{2} & -\frac{L}{2} & 0 & \frac{L}{2} & -\frac{L}{2} & 0 & -\frac{L}{2} & -\frac{L}{2} & 0 & \frac{L}{2} \\ 0 & -\frac{L}{2} & -\frac{L}{2} & \frac{L}{2} & -\frac{L}{2} & 0 & -\frac{L}{2} & \frac{L}{2} & 0 & 0 & \frac{L}{2} & -\frac{L}{2} \end{bmatrix} \tag{20}$$

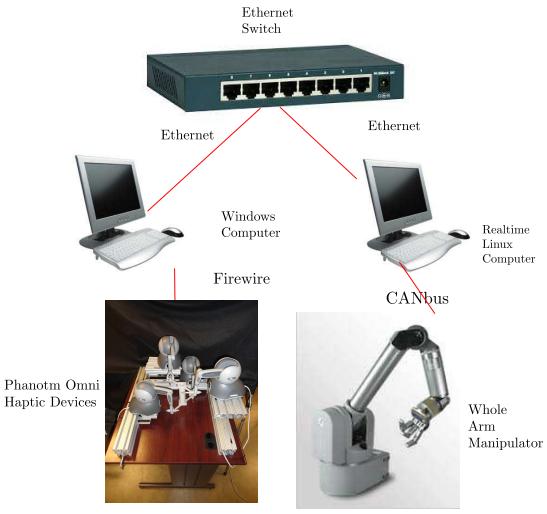

Fig. 5: Framework of Teleoperation Control System

Where P_o is the point where the haptic device enters the virtual wall in VE, θ_o is the orientation of the device when it enters the virtual wall, and k_t and k_p are the wall's translational and rotational stiffness, respectively. The force and torque profiles are shown in Fig. 7. As is shown in the figure, the force applied on the handle exceeded the capability we proposed.

VI. CONCLUSIONS AND FUTURE WORKS

A novel 6 DOF haptic device is proposed in this paper. Its kinematics and force control are discussed. Its actuation redundancy issue is also addressed. This device provides a large workspace, great force feedback and a low built cost. A haptic and a teleoperation experiment are presented to demonstrate its capability.

Other mechanisms can also be added to this system in future works to extend its functionality. For example, forceps can be installed to control the motion of any robot end effector such as robotic hands, or forceps. These different end-effectors can bring a variety of potential applications to our new haptic system, such as telesurgery or radioactive material remote handling. In haptics research, a 6 DOF force feedback can help the operator interact with the virtual environment better than haptics devices with less degrees of freedom. For instance, when simulating the process of using an electric drill to drill a hole in a stiff object, torque feedback is the major portion of the haptic feedback. Therefore, a 6 DOF master controller would provide a lot more information than 3 DOF master controllers.

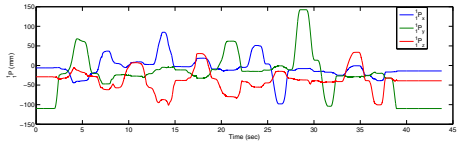

(a) Position of Phantom P1

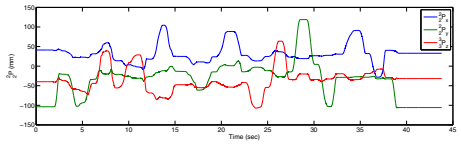

(b) Position of Phantom P2

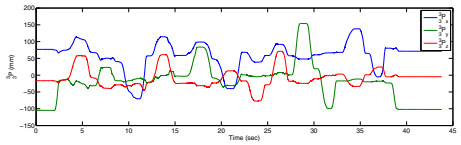

(c) Position of Phantom P3

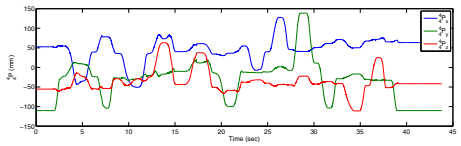

(d) Position of Phantom P4

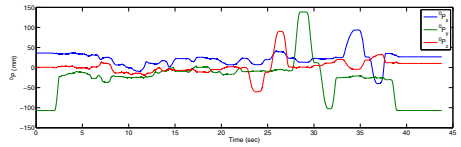

(e) Position of the Handle

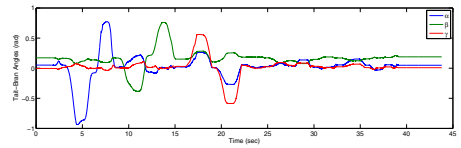

(f) Orientation of the Handle α stands for the euler angle w. r. t. the x axis, β represents the angle w. r. t. the y axis and γ represents the angle w. r. t. the z axis.

Fig. 6: Position and Orientation of the Omnis and the Handle

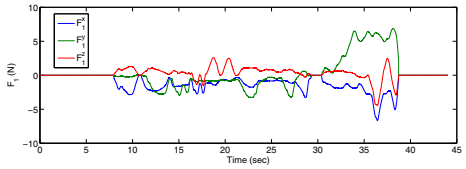

(a) Force Applied by Phantom P1

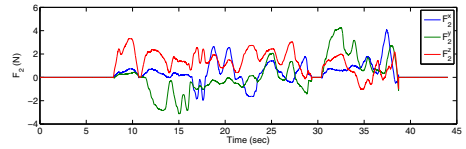

(b) Force Applied by Phantom P2

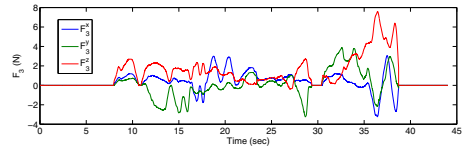

(c) Force Applied by Phantom P3

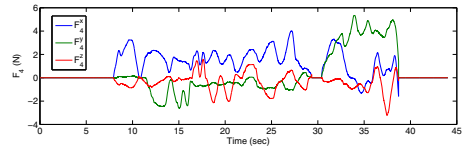

(d) Force Applied by Phantom P4

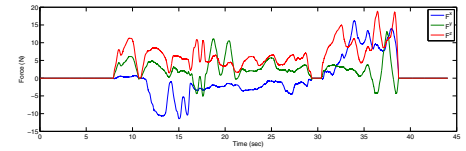

(e) Force Applied on the Handle

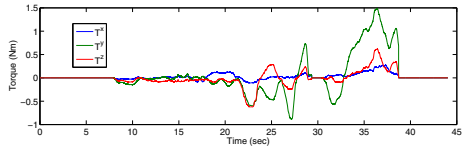

(f) Torque Applied on the Handle

Fig. 7: Force and Torque Feedback Profile

ACKNOWLEDGMENT

The authors would like to acknowledge the support of the U. S. National Science Foundation (grant 0844890). The author would also like to thank Mr. William Anderson and Mr. Daniel Graham for their support in manufacturing the proposed device.

REFERENCES

[1] F. Dimension. (2014) Force dimension products. [Online]. Available: http://www.forcedimension.com/products

[2] Quanser. (2014) Haptics wand. [Online]. Available: http://www.quanser.com/products/5dof-wand

[3] Geomagic. (2014) Phantom premium. [Online]. Available: http://www.geomagic.com/en/products/phantom-premium-6dof/overview

[4] Y. Tsumaki, H. Naruse, D. N. Nenchev, and M. Uchiyama, "Design of a compact 6-dof haptic interface," in *Robotics and Automation, 1998. Proceedings. 1998 IEEE International Conference on*, vol. 3. IEEE, 1998, pp. 2580–2585.

[5] K. Y. Woo, B. D. Jin, and D.-S. Kwon, "A 6-dof force-reflecting hand controller using the fivebar parallel mechanism," in *Robotics and Automation, 1998. Proceedings. 1998 IEEE International Conference on*, vol. 2. IEEE, 1998, pp. 1597–1602.

[6] A. Talvas, M. Marchal, C. Nicolas, G. Cirio, M. Emily, and A. Lécuyer, "Novel interactive techniques for bimanual manipulation of 3d objects with two 3dof haptic interfaces," in *Haptics: Perception, Devices, Mobility, and Communication*. Springer, 2012, pp. 552–563.

[7] M. H. Vu and U. J. Na, "A new 6-dof haptic device for teleoperation of 6-dof serial robots," *Instrumentation and Measurement, IEEE Transactions on*, vol. 60, no. 11, pp. 3510–3523, 2011.

[8] A. V. Shah, S. Teuscher, E. W. McClain, and J. J. Abbott, "How to build an inexpensive 5-dof haptic device using two novint falcons," in *Haptics: Generating and Perceiving Tangible Sensations*. Springer, 2010, pp. 136–143.

[9] Y. Lin and Y. Sun, "5-d force control system for fingernail imaging calibration," in *Robotics and Automation (ICRA), 2011 IEEE International Conference on*. IEEE, 2011, pp. 1374–1379.

[10] L.-W. Sun, F. Van Meer, Y. Bailly, and C. K. Yeung, "Design and development of a da vinci surgical system simulator," in *Mechatronics and Automation, 2007. ICMA 2007. International Conference on*. IEEE, 2007, pp. 1050–1055.

[11] A. Talvas, M. Marchal, G. Cirio, and A. Lécuyer, "3d interaction techniques for bimanual haptics in virtual environments," in *Multi-finger Haptic Interaction*. Springer, 2013, pp. 31–53.

[12] A. J. Silva, O. A. D. Ramirez, V. P. Vega, and J. P. O. Oliver, "Phantom omni haptic device: Kinematic and manipulability," in *Electronics, Robotics and Automotive Mechanics Conference, 2009. CERMA'09.* IEEE, 2009, pp. 193–198.

[13] M. C. Çavuşoğlu, D. Feygin, and F. Tendick, "A critical study of the mechanical and electrical properties of the phantom haptic interface and improvements for highperformance control," *Presence: Teleoperators and Virtual Environments*, vol. 11, no. 6, pp. 555–568, 2002.

[14] S. Technology, "Phantom omin user guide," SensAble Technologies, Inc., Tech. Rep., 2008.

[15] T. T. Soong, *Fundamentals of probability and statistics for engineers*. Wiley. com, 2004.

[16] S. P. Boyd and L. Vandenberghe, *Convex optimization*. Cambridge university press, 2004.

[17] E. Naerum and B. Hannaford, "Global transparency analysis of the lawrence teleoperator architecture," in *Robotics and Automation, 2009. ICRA'09. IEEE International Conference on*. IEEE, 2009, pp. 4344–4349.

[18] J. Kim, P. H. Chang, and H.-S. Park, "Transparent teleoperation using two-channel control architectures," in *Intelligent Robots and Systems, 2005.(IROS 2005). 2005 IEEE/RSJ International Conference on*. IEEE, 2005, pp. 1953–1960.

[19] J. E. Speich, K. Fite, and M. Goldfarb, "Transparency and stability robustness in two-channel bilateral telemanipulation," *Transactions of the ASME*, vol. 123, pp. 400–4007, 2001.

[20] D. Lee and K. Huang, "On passive non-iterative varying-step numerical integration of mechanical systems for haptic rendering," in *ASME Dynamic Systems & Control Conf*, 2008.